View metadata, citation and similar papers at core.ac.uk

brought to you by CORE

provided by Carolina Digital Repository

JVI Journals.ASM.org

A Cluster of Virus-Encoded MicroRNAs Accelerates Acute Systemic Epstein-Barr Virus Infection but Does Not Significantly Enhance Virus-Induced Oncogenesis *In Vivo*

Angela Wahl,[a] Sarah D. Linnstaedt,[b]* Caitlin Esoda,[b] John F. Krisko,[a] Francisco Martinez-Torres,[a]* Henri-Jacques Delecluse,[c] Bryan R. Cullen,[b] J. Victor Garcia[a]

Division of Infectious Diseases, Center for AIDS Research, University of North Carolina at Chapel Hill, School of Medicine, Chapel Hill, North Carolina, USA[a]; Center for Virology and Department of Molecular Genetics and Microbiology, Duke University Medical Center, Durham, North Carolina, USA[b]; Department of Virus Associated Tumours, German Cancer Research Center, Heidelberg, Germany[c]

Over 90% of the adult human population is chronically infected with the Epstein-Barr virus (EBV), an oncogenic herpesvirus. EBV primarily infects naive human B cells and persists latently in memory B cells. Most individuals experience an asymptomatic infection that is effectively controlled by the adaptive immune response. However, EBV-associated lymphomas can develop in immunocompromised individuals. These tumors typically express all nine EBV latent proteins (latency III). Latency III is also associated with the expression of three precursor microRNAs (miRNAs) located within the EBV BHRF1 gene locus. The role of these BHRF1 miRNAs was unclear until recent *in vitro* studies demonstrated that they cooperate to enhance virus-induced B cell transformation and decrease the antigenic load of virus-infected cells, indicating that the BHRF1 miRNA cluster may serve as a novel therapeutic target for the treatment of latency III EBV-associated malignancies. However, to date, it is not known if BHRF1 miRNAs enhance virus-induced oncogenesis and/or immune evasion of EBV *in vivo*. To understand the *in vivo* contribution of the BHRF1 miRNA cluster to EBV infection and EBV-associated tumorigenesis, we monitored EBV infection and assessed tumor formation in humanized mice exposed to wild-type virus and a viral mutant (Δ123) that lacks all three BHRF1 miRNAs. Our results demonstrate that while the BHRF1 miRNAs facilitate the development of acute systemic EBV infection, they do not enhance the overall oncogenic potential of EBV *in vivo*.

Epstein-Barr Virus (EBV), a human gamma herpesvirus, is widespread in all populations; more than 90% of adults worldwide have antibodies to EBV, and infection with EBV persists for the life of its host (1). In healthy individuals, EBV is effectively controlled by the immune system and typically remains asymptomatic. Upon primary infection, virus-targeted B cells undergo a period of rapid proliferation until either $CD8^+$ T cells mount an efficient antiviral response (2) or infected B cells differentiate into a pool of latently infected memory-like B cells (3). When the immune system is suppressed, EBV can induce the development of certain lymphomas (4–6).

EBV-associated malignancies that arise in immunodeficient individuals (i.e., posttransplant and AIDS patients) typically express all nine EBV latent proteins (latency III): six Epstein-Barr virus nuclear antigens (EBNA) and three latent membrane proteins (LMP) (1, 3). Although most EBV-associated malignancies respond poorly to chemotherapy, immunotherapy approaches that boost or supplement the patient's EBV-specific T cell response have been successful in treating some latency III tumors due to their high antigenic load (4). However, these strategies, which typically involve the adoptive transfer of autologous or allogeneic EBV-specific T cells stimulated *in vitro*, are often laborious and technically challenging (4). Therefore, new therapeutic targets and approaches are urgently needed for the treatment of EBV-associated malignancies.

In addition to the nine virus-encoded latent proteins, during latency III, EBV-transformed B cells also express a cluster of three precursor microRNAs (miRNAs) located within the EBV BHRF1 gene locus (1, 7). miRNAs are a class of RNAs 21 to 23 nucleotides (nt) long that posttranscriptionally regulate gene expression by binding to target sites on complementary mRNAs (8). Two of the three BHRF1 miRNAs are located in the BHRF1 3′ untranslated region and one is located immediately 5′ to the BHRF1 lytic mRNA transcription start site (7, 9). The roles of these BHRF1 miRNAs were unclear until recent *in vitro* studies using viral knockouts in lymphoblastoid cell lines (LCLs), a widely used cellular model of latency III EBV infection, revealed that the BHRF1 miRNAs cooperate to enhance B cell expansion, reduce levels of latent gene expression, and possibly also inhibit apoptosis (10–12). Additionally, as circumstantial evidence for the roles of these miRNAs, studies that comprehensively examined the targets of EBV miRNAs have shown that BHRF1 miRNAs bind a number of targets involved in proliferation, latent gene expression, and regulation of apoptosis (13, 14).

Collectively, these *in vitro* studies demonstrate that BHRF1 miRNAs cooperate to expand the viral reservoir and decrease the antigenic load and suggest that the BHRF1 miRNA cluster could

Received 29 January 2013 **Accepted** 26 February 2013

Published ahead of print 6 March 2013

Address correspondence to Bryan R. Cullen, bryan.cullen@duke.edu, or J. Victor Garcia, victor_garcia@med.unc.edu.

* Present address: Sarah D. Linnstaedt, Department of Anesthesiology, University of North Carolina at Chapel Hill, Chapel Hill, North Carolina, USA; Francisco Martinez-Torres, Department of Neurology, Krankenhaus Nordwest, Frankfurt, Germany.

Copyright © 2013, American Society for Microbiology. All Rights Reserved.

doi:10.1128/JVI.00281-13

serve as a novel therapeutic target for the treatment of latency III EBV-associated malignancies. However, to date, it is not known if BHRF1 miRNAs enhance the oncogenic potential and/or enhance immune evasion of EBV *in vivo*. Here, we utilized a humanized mouse model of EBV infection and tumorigenesis to examine the *in vivo* role of BHRF1 miRNAs. Until recently, *in vivo* studies with EBV have been limited; EBV exhibits very restricted species tropism (humans and New World primates such as the common marmoset and cottontop tamarin) (15, 16). Humanized mice generated by transplanting $CD34^+$ hematopoietic stems cells into immune-deficient mice devoid of mouse lymphoid cells are systemically reconstituted with human myeloid and lymphoid cells, including human B cells (the primary target cell of EBV) (17). EBV infection of humanized mice recapitulates several key aspects of human infection, including a virus-specific $CD8^+$ T cell immune response and the development of latency III EBV-associated tumors (18–20). To understand the *in vivo* contribution of the BHRF1 miRNA cluster to EBV infection and EBV-induced tumorigenesis, we monitored EBV infection and assessed tumor formation in humanized mice exposed to wild-type (WT) virus, a viral mutant (Δ123) that lacks all three BHRF1 miRNAs, and a revertant (REV) virus that was created by reexchanging the original BHRF1 miRNA sequences back into the Δ123 mutant (11). Our results demonstrate that while the BHRF1 miRNAs facilitate the development of acute systemic EBV infection, they do not enhance the overall oncogenic potential of EBV *in vivo*.

MATERIALS AND METHODS

EBV production and titer quantification. Viral particles were produced from HEK293 cells harboring a hygromycin-resistant, green fluorescent protein (GFP)-expressing, B95.8 EBV bacmid as described previously (21). Briefly, bacmid-containing cells were transfected with BZLF1- and gp110-expressing plasmids using Fugene (Roche, Indianapolis, IN) and the manufacturer's protocol (21, 22). Two days postinfection, cell supernatants containing viral particles were passed through 0.45-μm-pore-size filters and concentrated in Amicon Ultra-15 centrifugal filter units (Millipore, Billerica, MA). Virus titers were determined using green Raji units (GRU) (23). For each set of mouse exposures, we utilized virus stocks (WT, REV, and Δ123) that were prepared on the same day. Titers of virus stocks were determined in the same Raji cells on the same day. Frozen aliquots of virus were used for titration so as to mimic those utilized for exposures.

Preparation of humanized mice. Hematopoietic $CD34^+$ stem cells were isolated from enzymatically digested human fetal liver tissue by positive immunomagnetic isolation as previously described (24). Humanized mice were prepared by transplanting human fetal liver-derived hematopoietic $CD34^+$ stem cells (2×10^5 to 3.5×10^5 cells per mouse) intrahepatically into sublethally irradiated (100 cGy) 1-day-old NOD.Cg-Prkdc^{scid} IL2rγ^{tm1Wjl}/SzJ (NSG; The Jackson Laboratory, Bar Harbor, ME) mice. Reconstitution with human hematopoietic cells was monitored in peripheral blood by flow cytometry every 3 to 4 weeks as previously described (24). Mice were maintained under specific-pathogen-free conditions by the Division of Laboratory Animal Medicine at the University of North Carolina (UNC) at Chapel Hill.

EBV exposure of humanized mice. Humanized mice were challenged with 3.6×10^5 GRU of WT, REV or Δ123 EBV by injecting virus directly into the spleen (up to a 225-μl total volume) as previously described (24, 25). Briefly, mice were anesthetized and prepared for surgery, and a small incision was made on the left side of the abdomen to expose the spleen. If necessary, viral stocks were diluted with plain RPMI tissue culture medium immediately prior to exposure to ensure that an equivalent inoculum dose and volume were injected into each mouse. Following exposure, the incision site was sutured closed, and mice were allowed to fully recover from surgery. Two sets of splenic exposures were performed and with different preparations of virus.

Analysis of EBV infection in humanized mice. EBV infection in humanized mice was monitored in peripheral blood by measuring the levels of viral DNA in plasma and cells with a real-time PCR assay using the forward and reverse primers 5′-GGAACCTGGTCATCCTTGC-3′ and 5′-ACGTGCATGGACCGGTTAAT-3′, respectively, and the probe 5′-FAM-CGCAGGCACTCGTACTGCTCGCT-Q-3′ (where FAM is 6-carboxyfluorescein and Q is 6-carboxytetramethylrhodamine); the assay limit of detection was 375 DNA copies/ml (cell-associated EBV DNA) or 560 DNA copies/ml (cell-free EBV DNA) (26). The expansion, memory phenotype, and activation status of human $CD8^+$ T cells were monitored in peripheral blood pre- and postexposure by flow cytometry.

Mice were euthanized at 18 weeks postexposure or earlier if they experienced greater than 20% weight loss and/or appeared moribund, and a necropsy was performed to assess the presence of tumors. Tumors were harvested, snap-frozen, and stored at −80°C for subsequent nucleic acid extraction and real-time PCR analysis. Tumor images were taken with an iSight color camera, and the white balance and brightness were adjusted in Adobe Photoshop CS5.

RNA isolation from mouse tumors and real-time PCR of EBV latent genes and BHRF1 miRNAs. RNA was isolated from mouse tumors using TRIzol reagent according to the manufacturer's protocol (Life Technologies, Grand Island, NY). The quality and quantity of the RNA were measured using a Nanodrop 2000 (Thermo Scientific, Wilmington, DE), and the RNA was used for reverse transcription. For cDNA from mRNA, 500 ng of total RNA was used for reverse transcription using random primers and a High Capacity cDNA Reverse Transcription kit (Applied Biosystems, Carlsbad, CA). EBNA2 and LMP1 were detected via quantitative PCR (qPCR) using SYBR chemistry, a StepOnePlus machine (Applied Biosystems, Carlsbad, CA) and the following primers: EBNA2, 5′-GCTTAGCCAGTAACCCAGCACT-3′ (forward) and 5′-TGCTTAGAAGGTTGTTGGCATG-3′ (reverse); LMP1, 5′-AATTTGCACGGACAGGCATT-3′; (forward) and 5′-AAGGCCAAAAGCTGCCAGAT-3′ (reverse). Relative levels of EBNA2 and LMP1 were quantified using beta-actin mRNA as an internal reference. For cDNA from miRNA, 10 ng of total RNA was used for reverse transcription using miRNA-specific primers (Applied Biosystems, Carlsbad, CA) and a TaqMan MicroRNA Reverse Transcription kit (Applied Biosystems, Carlsbad, CA). BHRF1 miRNAs were detected via qPCR using TaqMan chemistry, a StepOnePlus machine, and miRNA-specific primers (Applied Biosystems, Carlsbad, CA) (27, 28). RNU48 snoRNA was used as an internal reference to calculate the relative levels of BHRF1 miRNA expression.

Statistical analyses. Statistical analyses were performed in Prism, version 5 (Graph Pad, La Jolla, CA). We used a log rank Mantel-Cox test to compare the rates of viral DNA detection in the peripheral blood and survival between WT/REV and Δ123 EBV-exposed mice. A two-tailed Mann-Whitney U test was used to compare the peak cell-associated and cell-free viral loads and the mean percentages of human cell populations in the peripheral blood of WT, REV, and Δ123 EBV-exposed mice. We compared tumor incidence between WT/REV and Δ123 EBV-exposed mice with Fisher's exact test.

RESULTS

Reconstitution of humanized mice with human hematopoietic cells. Humanized mice were created by injecting human fetal liver-derived $CD34^+$ hematopoietic stem cells into the liver of sublethally irradiated 1-day-old NSG mice. The humanized mice generated for this study represented four different human donors. Systemic reconstitution of humanized mice with human hematopoietic cells ($CD45^+$) was confirmed in peripheral blood prior to exposure by flow cytometry (mean percentage of human $CD45^+$ cells ± standard deviation [SD] for WT virus-exposed mice, 43.8% ± 15.2%; for REV virus-exposed mice, 48% ± 6.2%; for Δ123 virus-exposed mice, 40.1% ± 15.2%) (Fig. 1A). In addition,

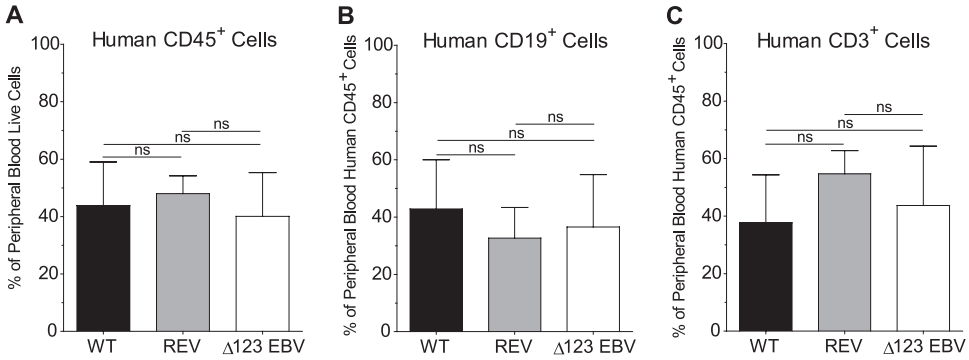

FIG 1 Reconstitution of humanized mice with human hematopoietic cells. Reconstitution of humanized mice with human hematopoietic cells was monitored in the peripheral blood by flow cytometry. The mean percentages of human hematopoietic cells ($CD45^+$), B cells ($CD19^+$), and T cells ($CD3^+$) in the peripheral blood of humanized mice prior to exposure to WT, REV or Δ123 EBV are shown. There was no significant difference in the percentages of human cells in the peripheral blood of mice exposed to WT, REV, or Δ123 EBV (two-tailed Mann-Whitney U test, significance defined as $P \leq 0.05$).

we also verified systemic reconstitution of mice with human B cells ($CD19^+$) (mean percentage of human $CD19^+$ ± SD for WT virus-exposed mice, 42.9% ± 17.1%; for REV virus-exposed mice, 32.7% ± 10.7%; for Δ123 virus-exposed mice, 36.5% ± 18.2%) and human T cells ($CD3^+$) (mean percentage of human $CD3^+$ ± SD for WT virus-exposed mice, 37.7% ± 16.6%; for REV virus-exposed mice, 54.7% ± 8.1%; for Δ123 virus-exposed mice, 43.7% ± 20.6%) (Fig. 1B and C). We observed no significant difference in the percentages of human hematopoietic cells, B cells, or T cells in peripheral blood of mice exposed to WT, REV, or Δ123 virus (Fig. 1).

Systemic EBV infection in WT/REV and Δ123 virus-exposed mice. Once we established systemic reconstitution of mice with human hematopoietic cells, we exposed humanized mice to WT, REV, or Δ123 EBV by injecting virus directly into the spleen. We then monitored systemic EBV infection by measuring peripheral blood viral load levels with real-time PCR. As expected from the nature of and *in vitro* characterization of the REV virus, we detected no significant *in vivo* differences in EBV infection between mice exposed to the WT and REV viruses (data not shown). Therefore, for the remainder of this report, we analyze the results generated from WT and REV EBV-exposed mice together and compare them to those of Δ123 virus-exposed mice.

We observed a significant delay in the appearance of viral DNA (cell-associated and/or cell-free) in the peripheral blood of mice exposed to Δ123 virus in comparison to mice exposed to WT/REV EBV (Fig. 2). Viral DNA was readily detected in the peripheral blood of 5/10 (50%) WT/REV virus-exposed mice as early as 2 weeks postexposure. When we performed a PCR analysis of tissues harvested from a WT virus-exposed mouse negative for viral DNA in the peripheral blood at 2 weeks postexposure, we detected viral DNA in both the spleen and liver, indicating that these tissues are early sites of virus replication prior to the appearance of viremia (data not shown). We detected viral DNA in the peripheral blood of all remaining mice exposed to WT/REV virus by 4 weeks postexposure (Fig. 2). In contrast, we detected viral DNA in the peripheral blood of only 1/11 (9%) Δ123 virus-exposed mice at 2 weeks postexposure and in only 6/11 (54%) Δ123 EBV-exposed mice by 4 weeks postexposure (Fig. 2). We detected viral DNA in the peripheral blood of all mice exposed to Δ123 virus by 6 weeks postexposure (Fig. 2).

Following the initial appearance of viral DNA in peripheral blood of EBV-exposed mice, we were able to periodically detect cell-associated (Fig. 3A and C) and cell-free (Fig. 3B and D) viral DNA in peripheral blood cells and plasma, respectively, of WT/REV and Δ123 virus-infected mice throughout the experiment. In addition, although we observed a delay in the appearance of viral DNA in the peripheral blood of Δ123 virus-infected mice, we did not observe a significant difference in the peak cell-associated (Fig. 3E) or cell-free (Fig. 3F) viral loads between WT/REV and Δ123 virus-exposed mice with detectable viremia.

Collectively, these results reveal that systemic EBV infection is delayed in mice exposed to virus lacking the BHRF1 miRNA cluster, as determined by the appearance of viral DNA in peripheral blood following exposure. However, once systemic infection was established, we observed no significant difference in the peak cell-associated or cell-free peripheral blood viral loads of mice exposed to virus that does or does not possess the three BHRF1 miRNAs.

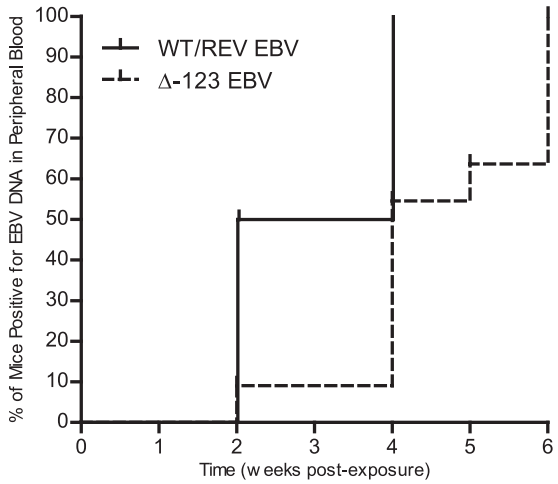

FIG 2 Detection of viral DNA in the peripheral blood of humanized mice exposed to EBV. Spleens of humanized mice were injected with 3.6×10^5 GRU of WT ($n = 7$), REV ($n = 3$), or Δ123 ($n = 11$) EBV. Following splenic exposure, infection was monitored in peripheral blood with real-time PCR. A Kaplan-Meier plot illustrates the week postexposure when EBV DNA was first detected in the peripheral blood of mice exposed to WT/REV or Δ123 EBV. The rate of viral DNA detection in the peripheral blood of mice exposed to WT/REV or Δ123 EBV was compared with a log rank Mantel-Cox test ($P = 0.0083$).

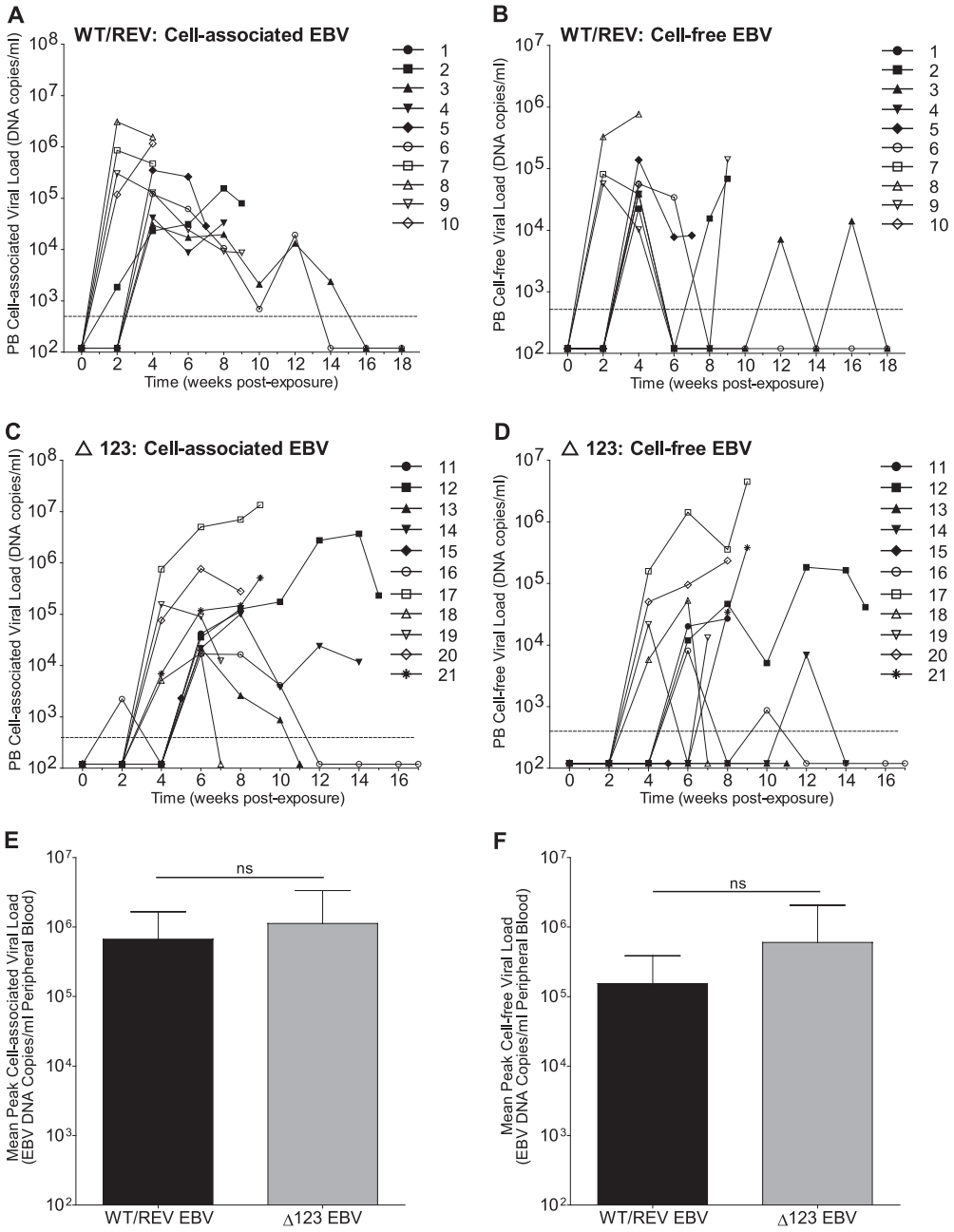

FIG 3 Detection of cell-associated and cell-free EBV DNA in the peripheral blood of EBV-exposed humanized mice. The presence of EBV DNA in peripheral blood cells (cell-associated DNA) and plasma (cell-free DNA) of WT/REV ($n = 10$) and Δ123 ($n = 11$) virus-exposed mice was determined with real-time PCR. The corresponding cell-associated (A and C) and cell-free (B and D) peripheral blood viral loads for each mouse are indicated with the same symbol. A dashed line indicates the assay limit of detection (cell-associated EBV DNA, 375 DNA copies/ml; cell-free EBV DNA, 560 DNA copies/ml). Cell-associated EBV DNA was detected in the peripheral blood of 9/10 WT/REV EBV-exposed mice and 11/11 Δ123 EBV-exposed mice. Cell-free EBV DNA was detected in the peripheral blood of 9/10 WT/REV EBV-exposed mice and 9/11 Δ123 EBV-exposed mice. There was no significant difference in the peak cell-associated (E) or cell-free (F) EBV viral loads in the peripheral blood of WT/REV and Δ123 EBV-exposed mice with detectable viremia (two-tailed Mann-Whitney U test; cell-associated, $P = 0.4964$; cell-free, $P = 0.6517$).

The effect of BHRF1 miRNAs on the peripheral blood CD8$^+$ T cell response during acute EBV infection. *In vivo*, acute EBV infection elicits a potent cell-mediated immune response that is characterized by peripheral blood CD8$^+$ T cell expansion, activation, and acquisition of a memory phenotype. While the CD8$^+$ T cell response primarily targets lytic viral proteins, particular latent proteins (EBNA1, EBNA3A, and EBNA3C) are also targeted by CD8$^+$ T cells during EBV infection. However, the magnitude of the CD8$^+$ T cell response to latent antigens during acute infection is less robust than the response to lytic antigens and peaks during convalescence (29). *In vitro*, BHRF1 miRNAs have been shown to reduce expression of latent viral proteins in infected B cells, which may facilitate immune evasion of latently infected B cells *in vivo* (30). B cells infected with the Δ123 mutant *in vitro* not only exhibit

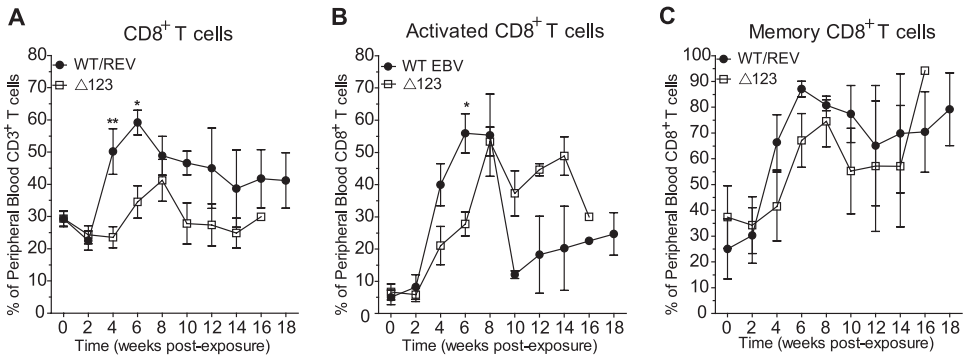

FIG 4 Expansion, activation, and memory phenotype of $CD8^+$ T cells in peripheral blood following EBV exposure. Flow cytometry was utilized to monitor the expansion, activation status, and memory phenotype of $CD8^+$ T cells in the peripheral blood of mice pre- and postexposure to WT/REV or Δ123 EBV. (A) The mean (± standard error of the mean) percentage of $CD3^+$ T cells that express CD8. (B) The mean (± standard error of the mean) percentage of activated ($CD38^+$ $HLA\text{-}DR^+$) $CD8^+$ T cells. (C) The mean (± standard error of the mean) percentage of memory ($CD45RA^-$) $CD8^+$ T cells. A two-tailed Mann-Whitney U test was used to compare the percentages of human $CD8^+$ T cells, activated $CD8^+$ T cells, and memory $CD8^+$ T cells in the peripheral blood of WT/REV and Δ123 EBV-exposed mice (*, $P \leq 0.05$; **, $P < 0.01$).

slower cell growth kinetics but also display increased expression of latent viral proteins compared to their WT/REV virus-infected counterparts (30). Therefore, we next wanted to examine the $CD8^+$ T cell response to EBV infection in the peripheral blood of mice exposed to the WT/REV and Δ123 viruses. We utilized flow cytometry to monitor the expansion, activation, and memory phenotype of $CD8^+$ T cells in the peripheral blood of mice pre- and postexposure to WT/REV and Δ123 EBV.

Although we observed an increase in the percentage of $CD8^+$ T cells in the peripheral blood of both WT/REV and Δ123 EBV-exposed mice during the course of infection, peripheral blood $CD8^+$ T cell expansion was significantly more robust in WT/REV virus-infected mice at 4 and 6 weeks postexposure than in mice infected with the Δ123 viral mutant (Fig. 4A). In addition, while $CD8^+$ T cell expansion in the peripheral blood peaked at week 6 postexposure during WT/REV virus infection, $CD8^+$ T cell expansion was delayed in Δ123 virus-infected mice and did not peak until 8 weeks postexposure (Fig. 4A). We also observed an increase in the percentage of activated $CD8^+$ T cells ($CD38^+$ $HLA\text{-}DR^+$) in the peripheral blood of mice following exposure to the WT/REV and Δ123 viruses (Fig. 4B). However, peripheral blood $CD8^+$ T cell activation was more pronounced in WT/REV virus-infected mice at early time points postexposure than in Δ123 virus-infected mice, reaching significance at 6 weeks postexposure (Fig. 4B). Although we observed a delay in peripheral blood $CD8^+$ T cell expansion and activation in mice infected with the Δ123 mutant, we did not observe a significant difference in the percentage of peripheral blood $CD8^+$ T cells exhibiting a memory phenotype ($CD45RA^-$) in mice infected with the WT/REV and Δ123 viruses (Fig. 4C). We observed an increase in the percentage of memory $CD8^+$ T cells in the peripheral blood of both WT/REV and Δ123 virus-infected mice (Fig. 4C). Memory (mean ± SD, 28.8% ± 29.67%; $n = 4$) and activated (4.15% ± 3.46%; $n = 2$) $CD8^+$ T cells were also detected in the peripheral blood of uninfected humanized mice, albeit at much lower levels than those observed in EBV-infected mice.

All together, these results indicate that mice infected with the WT/REV and Δ123 viruses exhibit peripheral blood $CD8^+$ T cell expansion, activation, and acquisition of a memory phenotype, mimicking the human condition. However, mice infected with virus lacking the BHRF1 miRNA cluster displayed reduced levels of peripheral blood $CD8^+$ T cell expansion and activation in comparison to their WT/REV virus-infected counterparts at early time points postexposure.

The *in vivo* contribution of BHRF1 miRNAs to EBV-induced tumorigenesis. In most individuals, EBV is effectively controlled by the immune system and establishes an asymptomatic chronic infection (1). However, EBV can induce the development of certain types of B cell lymphomas when the immune system is suppressed (5, 6). Although *in vitro* studies indicate that the BHRF1 miRNAs facilitate EBV-mediated B cell transformation (11), the extent to which these BHRF1 miRNAs contribute to EBV-induced tumorigenesis *in vivo* has not been investigated.

In order to assess the contribution of the BHRF1 miRNA cluster to EBV-induced tumor formation *in vivo*, we examined humanized mice infected with WT/REV and Δ123 EBV for the presence of tumors at 18 weeks postexposure or sooner if they experienced greater than 20% weight loss and/or appeared moribund. Although mice infected with the Δ123 viral mutant experienced a delay in the establishment of systemic EBV infection and in peripheral blood $CD8^+$ T cell expansion and activation, we observed no significant difference in the survival rates between mice infected with WT/REV and Δ123 EBV (Fig. 5). At necropsy, tumors were readily detected in multiple organs of both WT/REV and Δ123 EBV-infected mice and were most frequently observed in the spleen, liver, and kidney (Fig. 6 and Table 1). We also observed no significant difference in tumor incidence or tumor location between WT/REV and Δ123 EBV-infected mice (Fig. 6 and Table 1).

In vivo, EBV-associated tumors can be classified by the expression patterns of the nine EBV latent genes (i.e., latency status). BHRF1 miRNAs are expressed only in tumors that display latency III, which is characterized by the expression of all nine EBV latent genes (1, 7). Although other laboratories have reported that EBV-infected humanized mice generated via transplantation of human $CD34^+$ hematopoietic stem cells into NOG (NOD/Shi-scid/IL2Rγ^{null}) and NSG mice primarily develop tumors with latency III (18, 19), it is possible that our data are the result of the development of latency I and/or II tumors in WT/REV and/or Δ123 EBV-infected mice. Therefore, we determined the latency

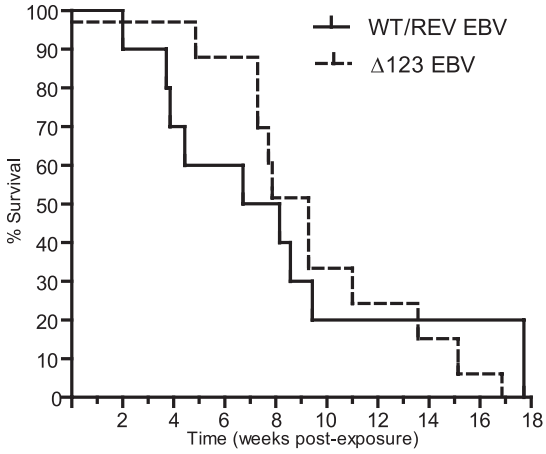

FIG 5 Survival rate of EBV-infected humanized mice. A Kaplan-Meier plot depicts the survival rate of mice exposed to either WT/REV or Δ123 EBV. The rates of survival between WT/REV and Δ123 EBV-exposed mice were compared with a log rank Mantel-Cox test ($P = 0.9171$).

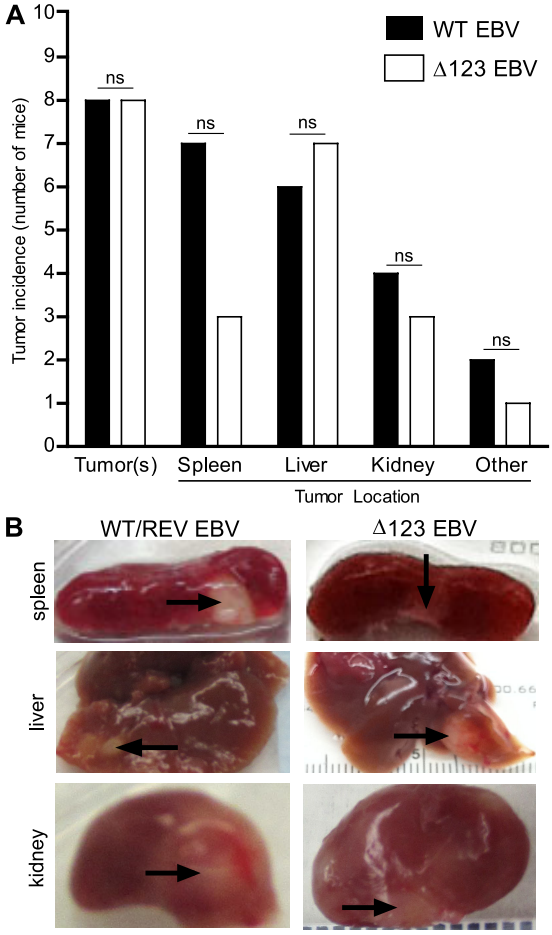

FIG 6 Tumor incidence in humanized mice exposed to WT/REV or Δ123 EBV. The presence and location of tumors in mice infected with WT/REV ($n = 9$) or Δ123 ($n = 11$) EBV were assessed at necropsy. (A) The number of WT/REV and Δ123 EBV-exposed mice with visible tumors at necropsy in the spleen, liver, kidney, and other organs. No significant (ns) difference in tumor incidence or tumor location was observed between WT/REV and Δ123 EBV-exposed mice at harvest (Fisher's exact test, significance defined as $P \leq 0.05$). (B) Images of the spleen, liver, and kidney of WT/REV and Δ123 EBV-exposed mice. Tumors are indicated with arrows.

status of tumors harvested from WT, REV, and Δ123 EBV-infected mice by determining their patterns of expression of the EBV latent genes LMP1 and EBNA2 with real-time PCR (latency I, LMP1$^-$ EBNA2$^-$; latency II, LMP1$^+$ EBNA2$^-$; latency III, LMP1$^+$ EBNA2$^+$) (6). All tumors analyzed from WT, REV and Δ123 EBV-infected mice expressed LMP1 and EBNA2 latency genes (latency III) (Fig. 7A). In addition, we also confirmed expression of BHRF1 miRNAs in the majority of tumors harvested from WT and REV virus-infected mice (Fig. 7B). Collectively, our results confirm that, in this humanized mouse system, EBV induces the formation of latency III tumors in multiple organs and demonstrate that BHRF1 miRNAs are expressed *in vivo* within these tumors. In addition, our data demonstrating no significant difference in the incidence, location, or latency status of tumors harvested from WT/REV and Δ123 EBV-infected mice indicate that the BHRF1 miRNA cluster does not enhance EBV-induced tumorigenesis *in vivo*.

DISCUSSION

In immune-compromising situations, EBV-induced B cell growth can cause lymphoproliferative disorders such as AIDS-associated lymphomas (e.g., diffuse large B cell lymphoma [DLBCL]) (31) and posttransplant lymphoproliferative disease (PTLD) (1). EBV in typical DLBCL and PTLD cells expresses all nine latent proteins (latency III) (1, 3). Studies in LCLs have shown that these latent proteins are necessary for EBV-induced B cell transformation (32–36). Recently, *in vitro* experiments have also indicated that during latency III, the B-cell-transforming properties of EBV are strongly potentiated by the virus-encoded BHRF1 miRNAs (11). In this study, we utilized a humanized mouse model of EBV infection and tumorigenesis to examine the contribution of BHRF1 miRNAs to the oncogenic potential of EBV *in vivo* in order to determine if these miRNAs may serve as an additional viral target for the therapeutic treatment of latency III EBV-associated malignancies.

Our *in vivo* results indicate that BHRF1 miRNAs accelerate the development of systemic EBV infection. Viremia was significantly delayed in humanized mice infected with the Δ123 mutant virus lacking the three BHRF1 miRNAs. The delay in viremia that we observed in Δ123 EBV-infected mice may be due to a lower growth rate of infected B cells. Previous *in vitro* experiments demonstrated that primary B cells infected with wild-type virus expanded more quickly than cells infected with Δ123 EBV. At 4 weeks postinfection, wild-type virus-infected B cells expanded from 2×10^6 cells to 3.6×10^8 cells while Δ123 EBV-infected cells expanded to only 1.3×10^8 cells (~3-fold fewer cells) (11). Although we observed a delay in the appearance of viral DNA in the peripheral blood of Δ123 EBV-infected mice, once viremia was established, we observed no significant difference in the peak viral loads between WT/REV and Δ123 EBV-infected mice. These results indicate that while BHRF1 miRNAs may accelerate expansion of infected B cells, B cells infected with virus lacking BHRF1 miRNAs are ultimately able to expand to similar levels as their wild-type virus-infected counterparts *in vivo*. Although we did not directly measure the amount of lytic viral replication in EBV-infected mice, our data demonstrating no significant difference between the peak cell-free and cell-associated viral loads of WT/

TABLE 1 Tumor incidence in EBV-infected mice

EBV	Mouse no.	Donor	Peripheral blood humanization at exposure by cell type (%)[a]			Peak viral load				Tumor incidence at harvest[e]				
						Cell-free		Cell-associated						
			$CD45^+$	$CD19^+$	$CD3^+$	No. of DNA copies/ml	Day	No. of DNA copies/ml	Day	Day	Spleen	Liver	Kidney	Other
WT	1[b]	C	61	12	60	ND[d]	14	ND	14	14[c]	−	−	−	−
	2	D	54	52	34	68,347	60	79,197	60	60	+	+	+	−
	3	D	49	40	39	38,892	28	30,174	28	124	−	+	+	−
	4	A	44	40	40	81,495	17	857,847	17	31	+	−	−	−
	5	A	48	47	40	768,867	27	3,087,704	17	27	+	+	−	+
	6	A	37	40	46	141,315	66	302,618	17	66	+	+	+	−
	7	B	14	69	5	928,928	36	1,161,146	27	36	+	+	−	+
REV	8	D	50	42	49	39,011	28	41,642	28	57	−	−	−	−
	9	C	41	21	64	138,293	28	352,638	28	47	+	+	+	−
	10	D	53	35	51	56,797	28	120,803	28	124	+	−	−	−
Δ123	11	C	47	32	49	26,780	54	113,798	54	54	+	+	−	−
	12	C	50	23	53	182,496	83	3,688,297	96	106	−	+	−	−
	13	C	34	17	65	ND	77	21,988	42	77	+	+	−	−
	14	D	43	47	39	6,865	83	100,732	55	95	+	+	−	−
	15	D	64	55	30	ND	34	2,288	34	34	−	−	−	−
	16	D	34	37	52	8,083	42	16,766	42	118	−	−	−	−
	17	A	60	18	68	21,759	28	154,749	28	51	−	−	−	−
	18	B	15	60	1	234,490	55	765,365	42	55	−	+	+	−
	19	B	28	64	19	4,494,995	65	13,414,096	65	65	−	+	+	−
	20	A	44	38	42	52,774	42	17,540	42	51	−	+	−	−
	21	A	22	11	63	380,633	65	513,500	65	65	−	−	+	+

[a] Gating strategy: live → $hCD45^+$ → $hCD19^+$ or $hCD3^+$ (where h is human).
[b] Not included in tumor analyses.
[c] EBV DNA detected in spleen and liver at harvest.
[d] ND, not detected.
[e] Presence (+) or absence (−) of tumor(s) is indicated.

REV and Δ123 EBV-infected mice also suggest that the delay in viremia observed following Δ123 EBV exposure is not due to decreased lytic viral replication.

Robust killing of EBV-infected cells by virus-specific $CD8^+$ T cells could also account for a delay in the appearance of viremia during Δ123 EBV infection. Previously published *in vitro* studies revealed that B cells infected with Δ123 virus expressed higher levels of the viral proteins expressed during latency III, including those most commonly targeted by $CD8^+$ T cells (EBNA1, EBNA3A, and EBNA3C) (11, 29). It is therefore possible that increased antigen presentation makes Δ123 virus-infected cells more susceptible to CD8 T cell killing *in vivo* and that the delay in the appearance of viral DNA in peripheral blood that we observed during Δ123 virus infection is due to increased killing of infected cells. Contradicting this rationale was the observation of significantly less $CD8^+$ T cell proliferation and activation in the peripheral blood of Δ123 virus-infected mice than in mice infected with WT/REV virus at early time points postexposure (week 4 and/or 6 postexposure). In this study, limited sample volume (~150 μl of blood per mouse) precluded a longitudinal analysis of the EBV-specific T cell response (i.e., tetramer staining, cytotoxicity assays, etc) following exposure. However, our *in vivo* data combined with previously published *in vitro* studies demonstrating decreased growth of Δ123 virus-infected cells suggest that decreased growth and not increased killing of infected cells decreases the reservoir of virus-infected cells, thereby delaying the detection of viremia in mice infected with virus lacking the BHRF1 miRNAs. In addition, these data indicate that the decreased peripheral blood $CD8^+$ T cell proliferation and activation that we observed following Δ123 virus infection is most likely due to a lower level of EBV-infected cells present systemically at early time points postexposure.

Although viral mutants lacking the EBV latent protein EBNA1, EBNA2, EBNA-LP, or LMP-1 exhibit a drastic reduction in their ability to transform B cells (32–36), it is not known if these proteins are sufficient for B cell transformation *in vivo* or if other virus-encoded components contribute to the transforming potential of EBV. One of our goals here was to determine if the virus-encoded BHRF1 miRNAs significantly promote EBV-induced oncogenesis *in vivo* given their documented ability to enhance B cell transformation *in vitro* (11). Therefore, we exposed humanized mice to WT/REV EBV or virus lacking the three BHRF1 miRNAs (Δ123 EBV) and subsequently monitored survival and tumor formation. Although Δ123 EBV exhibits a reduced capacity to transform B cells *in vitro*, we did not observe a significant difference in survival or tumor formation between mice exposed to WT/REV and Δ123 EBV. At necropsy, we consistently observed tumors in EBV-infected mice (88% of WT/REV and 73% of Δ123 virus-infected mice). Several WT/REV and Δ123 EBV-infected mice possessed tumors in multiple organs, most commonly the liver, spleen, and kidney, which is consistent with what other investigators have reported in this humanized EBV mouse model (18, 19). We also confirmed LMP1 and EBNA2 expression in all tumors

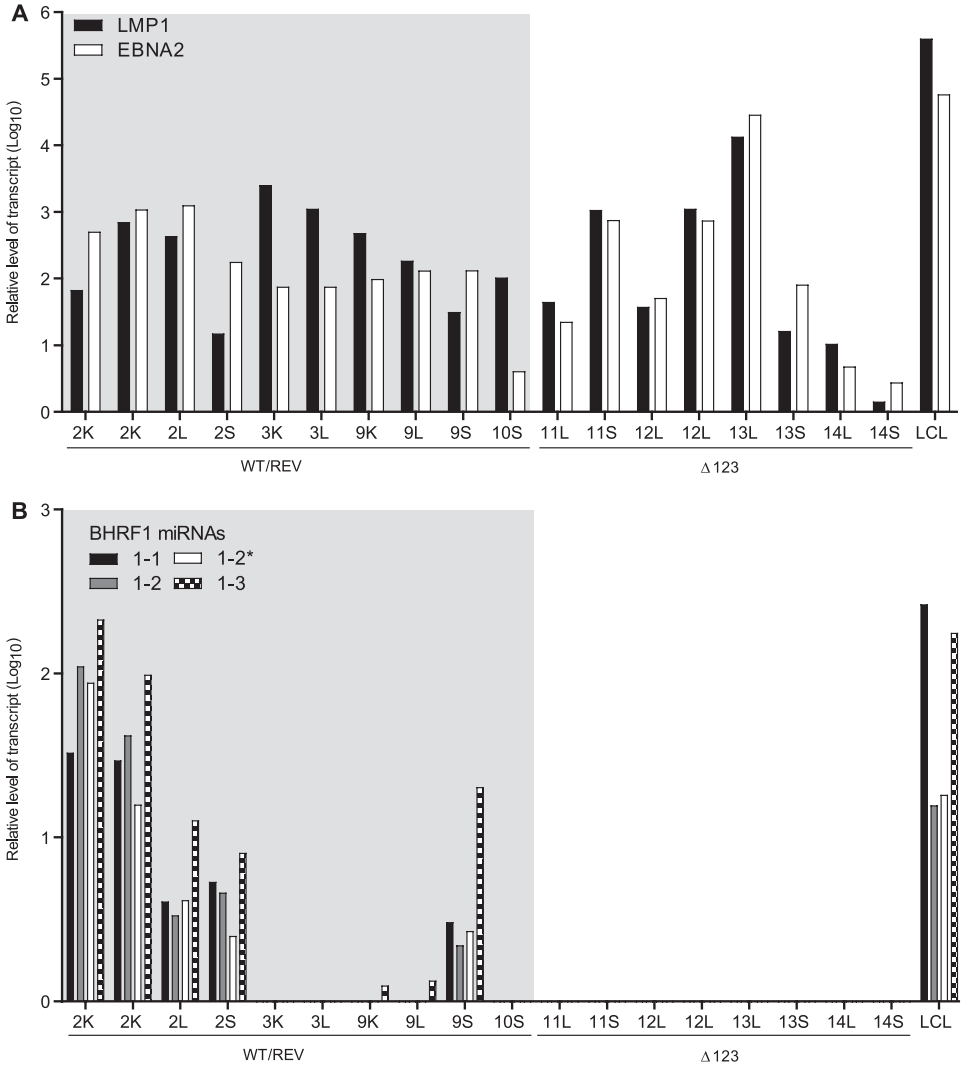

FIG 7 Expression of EBV latent proteins and BHRF1 miRNAs in tumors harvested from EBV-infected mice. We analyzed tumors harvested from four WT/REV and four Δ123 EBV-infected mice to assess latency status (A) and BHRF1 miRNA expression (B). The corresponding mouse number and location (S, spleen; L, liver; K, kidney) of each tumor are indicated. Latency status was determined by the relative expression level of EBV latent proteins LMP1 and EBNA2 and was defined as follows: latency I, $LMP1^-$ $EBNA2^-$; latency II, $LMP1^+$ $EBNA2^-$; and latency III, $LMP1^+$ $EBNA2^+$. The relative expression level of each BHRF1 miRNA is also indicated (the typically less abundant of the two possible BHRF1-2 miRNAs is noted with an asterisk). LCLs were used as a positive control for latency III and BHRF1 miRNA expression.

analyzed from WT/REV and Δ123 EBV-infected mice, characteristic of latency III EBV infection. In addition, we detected expression of one or more of the three BHRF1 miRNAs in the majority of tumors isolated from WT/REV EBV-infected mice (70%) and confirmed the absence of BHRF1 miRNAs in tumors harvested from Δ123 virus-infected mice. Collectively, these results indicate that latency III EBV-associated malignancies can develop *in vivo* in the presence or absence of BHRF1 miRNAs.

Although we detected expression of both LMP1 and EBNA2 in all tumors analyzed from EBV-infected mice, which is characteristic of latency III, we did not detect BHRF1 miRNA expression in all tumors analyzed from WT/REV EBV-infected mice (30%). It is possible that our inability to detect BHRF1 miRNA expression could be due to a mixture of latency I/II and III EBV-infected B cells within these tumors. BHRF1 miRNAs are not expressed during latency I or II (7), and the presence of latency I/II EBV-infected B cells within these tumors could potentially decrease the overall level of BHRF1 miRNA expression. While we cannot rule out that latency I or II EBV-infected B cells are not present within these tumors, or within tumors harvested from Δ123 virus-infected mice, we detected expression of both LMP1 and EBNA2 in all tumors analyzed, albeit at various levels. We also observed expression of both LMP1 and EBNA2 in LCLs, our positive control for latency III EBV infection and BHRF1 miRNA expression (Fig. 7). In addition, other laboratories have also reported that EBV infection induces the formation of latency III malignancies in this humanized mouse model (18, 19). Alternatively, our inability to detect BHRF1 miRNA expression in all tumors analyzed from WT/REV virus-infected mice may also indicate that, *in vivo*, the levels of BHRF1 miRNA expression vary among latency III tumors. In some instances, BHRF1 miRNA may be expressed at levels below our current limit of detection. Previous studies investigating

BHRF1 miRNA expression levels and function during latency III EBV infection utilized EBV-infected cell lines and *in vitro* EBV-transformed B cells (LCLs) (7, 10, 11, 37). Technical challenges in extracting tumors from surrounding noninfected tissue may also limit our ability to detect BHRF1 miRNA expression *in vivo*, especially in the case of smaller tumors. The presence of contaminating noninfected tissue may interfere with our ability to detect miRNA expression in tumor tissue. Nevertheless, despite these potential challenges, we were able to detect expression of one or more BHRF miRNAs in the majority of tumors analyzed from mice infected with WT/REV EBV. Collectively, our results reveal that the absence of BHRF1 miRNA expression does not impede the generation of latency III EBV-associated malignancies *in vivo*.

In conclusion, although we did not directly recapitulate previously published *in vitro* results demonstrating that Δ123 virus reduced transformation, we did observe a delay in the ability of Δ123 virus to cause systemic infection. The results of our *in vivo* analyses suggest that the mechanism for this delay is most likely due to decreased growth of infected cells. In addition, they also indicate that BHRF1 miRNAs are not required for the formation of latency III EBV-associated malignancies *in vivo* and that other viral components are able to compensate for the loss of BHRF1 miRNA activity during tumorigenesis.

ACKNOWLEDGMENTS

This research was supported by NIH grants R01-AI067968 (B.R.C.), T32-AI007273 (A.W.), and T32-AI007392 (S.D.L.) and by NCI supplemental funding for HIV-associated malignancy research to the UNC Lineberger Cancer Center and the UNC CFAR (J.V.G.).

We thank R.A. Spagnuolo for her technical assistance with the EBV viral load assays. We also thank current and past members of the laboratory for their contributions to this work.

REFERENCES

1. **Rickinson AB, Kieff E.** 2007. Epstein-Barr virus, p 2655–2700. *In* Knipe DM, Howley PM, Griffin DE, Lamb RA, Martin MA, Roizman B, Straus SE (ed), Fields virology, 5th ed, **vol 2**. Lippincott Williams & Wilkins, Philadelphia, PA.
2. **Rickinson AB, Callan MF, Annels NE.** 2000. T-cell memory: lessons from Epstein-Barr virus infection in man. Philos. Trans. R. Soc. Lond. B Biol. Sci. **355**:391–400.
3. **Thorley-Lawson DA.** 2005. EBV persistence and latent infection in vivo, p 309–357. *In* Robertson ES (ed), Epstein-Barr virus. Caister Academic Press, Wymondham, Norfolk, England.
4. **Heslop HE.** 2005. Biology and treatment of Epstein-Barr virus-associated non-Hodgkin lymphomas. Hematology Am. Soc. Hematol. Educ. Program **2005**:260–266.
5. **Munz C, Moormann A.** 2008. Immune escape by Epstein-Barr virus associated malignancies. Semin. Cancer Biol. **18**:381–387.
6. **Thorley-Lawson DA, Gross A.** 2004. Persistence of the Epstein-Barr virus and the origins of associated lymphomas. N. Engl. J. Med. **350**:1328–1337.
7. **Cai X, Schafer A, Lu S, Bilello JP, Desrosiers RC, Edwards R, Raab-Traub N, Cullen BR.** 2006. Epstein-Barr virus microRNAs are evolutionarily conserved and differentially expressed. PLoS Pathog. **2**:e23. doi:10.1371/journal.ppat.0020023.
8. **Bartel DP.** 2004. MicroRNAs: genomics, biogenesis, mechanism, and function. Cell **116**:281–297.
9. **Pfeffer S, Zavolan M, Grasser FA, Chien M, Russo JJ, Ju J, John B, Enright AJ, Marks D, Sander C, Tuschl T.** 2004. Identification of virus-encoded microRNAs. Science **304**:734–736.
10. **Feederle R, Haar J, Bernhardt K, Linnstaedt SD, Bannert H, Lips H, Cullen BR, Delecluse HJ.** 2011. The members of an Epstein-Barr virus microRNA cluster cooperate to transform B lymphocytes. J. Virol. **85**:9801–9810.
11. **Feederle R, Linnstaedt SD, Bannert H, Lips H, Bencun M, Cullen BR, Delecluse HJ.** 2011. A viral microRNA cluster strongly potentiates the transforming properties of a human herpesvirus. PLoS Pathog. **7**:e1001294. doi:10.1371/journal.ppat.1001294.
12. **Seto E, Moosmann A, Gromminger S, Walz N, Grundhoff A, Hammerschmidt W.** 2010. MicroRNAs of Epstein-Barr virus promote cell cycle progression and prevent apoptosis of primary human B cells. PLoS Pathog. **6**:e1001063. doi:10.1371/journal.ppat.1001063.
13. **Riley KJ, Rabinowitz GS, Yario TA, Luna JM, Darnell RB, Steitz JA.** 2012. EBV and human microRNAs co-target oncogenic and apoptotic viral and human genes during latency. EMBO J. **31**:2207–2221.
14. **Skalsky RL, Corcoran DL, Gottwein E, Frank CL, Kang D, Hafner M, Nusbaum JD, Feederle R, Delecluse HJ, Luftig MA, Tuschl T, Ohler U, Cullen BR.** 2012. The viral and cellular microRNA targetome in lymphoblastoid cell lines. PLoS Pathog. **8**:e1002484. doi:10.1371/journal.ppat.1002484.
15. **Shope T, Dechairo D, Miller G.** 1973. Malignant lymphoma in cottontop marmosets after inoculation with Epstein-Barr virus. Proc. Natl. Acad. Sci. U. S. A. **70**:2487–2491.
16. **Wedderburn N, Edwards JM, Desgranges C, Fontaine C, Cohen B, de The G.** 1984. Infectious mononucleosis-like response in common marmosets infected with Epstein-Barr virus. J. Infect. Dis. **150**:878–882.
17. **Shultz LD, Brehm MA, Garcia-Martinez JV, Greiner DL.** 2012. Humanized mice for immune system investigation: progress, promise and challenges. Nat. Rev. Immunol. **12**:786–798.
18. **Strowig T, Gurer C, Ploss A, Liu YF, Arrey F, Sashihara J, Koo G, Rice CM, Young JW, Chadburn A, Cohen JI, Munz C.** 2009. Priming of protective T cell responses against virus-induced tumors in mice with human immune system components. J. Exp. Med. **206**:1423–1434.
19. **Yajima M, Imadome K, Nakagawa A, Watanabe S, Terashima K, Nakamura H, Ito M, Shimizu N, Honda M, Yamamoto N, Fujiwara S.** 2008. A new humanized mouse model of Epstein-Barr virus infection that reproduces persistent infection, lymphoproliferative disorder, and cell-mediated and humoral immune responses. J. Infect. Dis. **198**:673–682.
20. **Yajima M, Imadome K, Nakagawa A, Watanabe S, Terashima K, Nakamura H, Ito M, Shimizu N, Yamamoto N, Fujiwara S.** 2009. T cell-mediated control of Epstein-Barr virus infection in humanized mice. J. Infect. Dis. **200**:1611–1615.
21. **Delecluse HJ, Hilsendegen T, Pich D, Zeidler R, Hammerschmidt W.** 1998. Propagation and recovery of intact, infectious Epstein-Barr virus from prokaryotic to human cells. Proc. Natl. Acad. Sci. U. S. A. **95**:8245–8250.
22. **Neuhierl B, Feederle R, Hammerschmidt W, Delecluse HJ.** 2002. Glycoprotein gp110 of Epstein-Barr virus determines viral tropism and efficiency of infection. Proc. Natl. Acad. Sci. U. S. A. **99**:15036–15041.
23. **Altmann M, Hammerschmidt W.** 2005. Epstein-Barr virus provides a new paradigm: a requirement for the immediate inhibition of apoptosis. PLoS Biol. **3**:e404. doi:10.1371/journal.pbio.0030404.
24. **Melkus MW, Estes JD, Padgett-Thomas A, Gatlin J, Denton PW, Othieno FA, Wege AK, Haase AT, Garcia JV.** 2006. Humanized mice mount specific adaptive and innate immune responses to EBV and TSST-1. Nat. Med. **12**:1316–1322.
25. **Islas-Ohlmayer M, Padgett-Thomas A, Domiati-Saad R, Melkus MW, Cravens PD, Martin Mdel P, Netto G, Garcia JV.** 2004. Experimental infection of NOD/SCID mice reconstituted with human $CD34^+$ cells with Epstein-Barr virus. J. Virol. **78**:13891–13900.
26. **Niesters HG, van Esser J, Fries E, Wolthers KC, Cornelissen J, Osterhaus AD.** 2000. Development of a real-time quantitative assay for detection of Epstein-Barr virus. J. Clin. Microbiol. **38**:712–715.
27. **Pratt ZL, Kuzembayeva M, Sengupta S, Sugden B.** 2009. The microRNAs of Epstein-Barr Virus are expressed at dramatically differing levels among cell lines. Virology **386**:387–397.
28. **Chen C, Ridzon DA, Broomer AJ, Zhou Z, Lee DH, Nguyen JT, Barbisin M, Xu NL, Mahuvakar VR, Andersen MR, Lao KQ, Livak KJ, Guegler KJ.** 2005. Real-time quantification of microRNAs by stem-loop RT-PCR. Nucleic Acids Res. **33**:e179. doi:10.1093/nar/gni178.
29. **Hislop AD, Taylor GS, Sauce D, Rickinson AB.** 2007. Cellular responses to viral infection in humans: lessons from Epstein-Barr virus. Annu. Rev. Immunol. **25**:587–617.
30. **Hutzinger R, Feederle R, Mrazek J, Schiefermeier N, Balwierz PJ, Zavolan M, Polacek N, Delecluse HJ, Huttenhofer A.** 2009. Expression and processing of a small nucleolar RNA from the Epstein-Barr virus genome. PLoS Pathog. **5**:e1000547. doi:10.1371/journal.ppat.1000547.
31. **Carbone A, Cesarman E, Spina M, Gloghini A, Schulz TF.** 2009. HIV-associated lymphomas and gamma-herpesviruses. Blood **113**:1213–1224.
32. **Cohen JI, Wang F, Mannick J, Kieff E.** 1989. Epstein-Barr virus nuclear

protein 2 is a key determinant of lymphocyte transformation. Proc. Natl. Acad. Sci. U. S. A. **86**:9558–9562.
33. **Hammerschmidt W, Sugden B.** 1989. Genetic analysis of immortalizing functions of Epstein-Barr virus in human B lymphocytes. Nature **340**: 393–397.
34. **Humme S, Reisbach G, Feederle R, Delecluse HJ, Bousset K, Hammerschmidt W, Schepers A.** 2003. The EBV nuclear antigen 1 (EBNA1) enhances B cell immortalization several thousandfold. Proc. Natl. Acad. Sci. U. S. A. **100**:10989–10994.
35. **Kaye KM, Izumi KM, Kieff E.** 1993. Epstein-Barr virus latent membrane protein 1 is essential for B-lymphocyte growth transformation. Proc. Natl. Acad. Sci. U. S. A. **90**:9150–9154.
36. **Mannick JB, Cohen JI, Birkenbach M, Marchini A, Kieff E.** 1991. The Epstein-Barr virus nuclear protein encoded by the leader of the EBNA RNAs is important in B-lymphocyte transformation. J. Virol. **65**:6826–6837.
37. **Qiu J, Cosmopoulos K, Pegtel M, Hopmans E, Murray P, Middeldorp J, Shapiro M, Thorley-Lawson DA.** 2011. A novel persistence associated EBV miRNA expression profile is disrupted in neoplasia. PLoS Pathog. **7**:e1002193. doi:10.1371/journal.ppat.1002193.